

Inversion-Recovery of Nitroxide Spin Labels in Solution and Microheterogeneous Environments

Igor V. Koptuyug,[†] Stefan H. Bossmann,[‡] and Nicholas J. Turro*[§]

Contribution from the Department of Chemistry, Columbia University, New York, New York 10027

Received June 30, 1995[⊗]

Abstract: Two modifications of a conventional inversion-recovery experiment which exclude the effect of spectral diffusion on the measured spin–lattice relaxation times of rapidly tumbling nitroxide spin labels are described. In the first approach an almost uniform inversion is achieved by means of specially designed pulse trains with excitation patterns which match the three-line nitroxide ESR spectrum. In the second approach we essentially combine an inversion-recovery for the $M_1 = 0$ line with an analog of a pulsed ELDOR technique for $M_1 = \pm 1$ lines in a single experiment. This allows us to reconstruct the recovery of the total magnetization of the ensemble of radicals which is not affected by spectral diffusion. The spin–lattice relaxation times of several nitroxide spin labels in different homogeneous and microheterogeneous environments are measured and compared. The temperature dependence of T_1 times is compared for two solvents, methylcyclohexane and carbon disulfide, which differ in nuclear spin concentration by almost a factor of 1000. The reported experimental evidence suggests that interactions with the nuclear spins of a solvent do not significantly contribute to the spin–lattice relaxation of nitroxide spin labels.

1. Introduction

In the last 30 years electron spin resonance (ESR) spectroscopy has been widely and successfully used in the studies of the structure, the internal mobility, and rotational and translational diffusion in various microheterogeneous systems of chemical and biological nature.^{1–3} One very instructive example of these endeavors is the evaluation of the correlation times of rotational reorientation of stable nitroxide radicals by studying the line shapes in their continuous wave (cw) ESR spectra. Many application examples^{4–8} have proven this approach to be highly reliable in the case of slow anisotropic tumbling of nitroxides. However, for fast isotropic tumbling conditions spin–lattice relaxation time measurements have a higher information content. Due to the recent developments in the field of pulsed ESR this latter approach is currently gaining popularity. As an extension of our studies of various microheterogeneous environments⁹ we have attempted to implement pulsed ESR—namely the inversion-recovery technique—for spin–lattice relaxation measurements of nitroxide spin labels. As a first step in this direction it is necessary to develop a reliable experimental protocol, since

applications of inversion-recovery technique to measure electron spin–lattice relaxation times of nitroxide radicals are relatively scarce.¹⁵

It is widely appreciated that spectral diffusion¹⁰ can lead to significant complications in spin–lattice relaxation measurements, if only a portion of an ESR spectrum is perturbed during the preparation period.^{11–15} For modern pulsed ESR instruments the typical microwave (mw) field magnitudes are insufficient to saturate or invert the entire motionally narrowed ESR spectrum of a nitroxide spin label. For example, for the Bruker ESP-380 instrument equipped with the dielectric ring cavity the effective mw field amplitude can be estimated as $B_1 \approx 5.6$ G in the rotating frame from the nominal 32-ns duration of the 180° pulse. The value of B_1 gives a rough estimate of the inversion bandwidth of a single 180° pulse, which is obviously much smaller than the spread of a nitroxide ESR spectrum. As a result, the evolution of a perturbed ESR line toward equilibrium is driven by both *true* spin–lattice relaxation and the redistribution of initial perturbation across the non-uniformly perturbed spectrum. Furthermore, the rates of both processes are environment-dependent, and thus a change in an apparent relaxation time T_1^{obs} does not necessarily imply a change in a true spin–lattice relaxation time T_1 . Such complications render the interpretation of the results in such experiments extremely difficult or impossible.

[†] Permanent address: Institute of Chemical Kinetics and Combustion, Novosibirsk 630090, Russia.

[‡] Present address: Lehrstuhl für Umweltmesstechnik, University of Karlsruhe, D-76128 Karlsruhe, Germany.

[⊗] Abstract published in *Advance ACS Abstracts*, January 1, 1996.

(1) Berliner, L. J., Ed. *Spin Labeling: Theory and Applications*; Academic Press: New York, 1979; Vol. 2.

(2) Berliner, L. J.; Reuben, J., Eds. *Biological Magnetic Resonance*; Plenum Press: New York/London, 1989; Vol. 8.

(3) Martini, G. *Colloids Surf.* **1990**, *45*, 83.

(4) Ottaviani, M. F.; Ghatlia, N. D.; Bossmann, S. H.; Barton, J. K.; Dürr, H.; Turro, N. J. *J. Am. Chem. Soc.* **1992**, *114*, 8946.

(5) Ottaviani, M. F.; Ghatlia, N. D.; Turro, N. J. *J. Phys. Chem.* **1992**, *96*, 6075.

(6) Winnik, F. M.; Ottaviani, M. F.; Bossmann, S. H.; Garcia-Garibay, M.; Turro, N. J. *Macromolecules* **1992**, *25*, 6007.

(7) Winnik, F. M.; Ottaviani, M. F.; Bossmann, S. H.; Pan, W.; Garcia-Garibay, M.; Turro, N. J. *Macromolecules* **1993**, *26*, 4577.

(8) Winnik, F. M.; Ottaviani, M. F.; Bossmann, S. H.; Pan, W.; Garcia-Garibay, M.; Turro, N. J. *J. Phys. Chem.* **1993**, *97*, 12998.

(9) Wu, C.-S.; Jenks, W. S.; Koptuyug, I. V.; Ghatlia, N. D.; Lipson, M.; Tarasov, V. F.; Turro, N. J. *J. Am. Chem. Soc.* **1993**, *115*, 9583 and references therein.

(10) We use the term “spectral diffusion” to refer to any process which transfers magnetization within the ensemble of spins, from one part of an ESR spectrum to another. Intra- and intermolecular mechanisms of spectral diffusion essential for nitroxide radicals in solution studied in this work are nuclear spin relaxation, Heisenberg spin exchange, and electron dipole–dipole interaction.

(11) Hyde, J. S. In *Time Domain Electron Spin Resonance*; Kevan, L., Schwartz, R. N., Eds.; Wiley-Interscience: New York, 1979; pp 1–30.

(12) Brown, I. M. In *Time Domain Electron Spin Resonance*; Kevan, L., Schwartz, R. N., Eds.; Wiley-Interscience: New York, 1979; pp 195–229.

(13) Thomann, H.; Dalton, L. R.; Dalton, L. A. In *Biological Magnetic Resonance*; Berliner, L. J., Reuben, J., Eds.; Plenum Press: New York/London, 1984; Vol. 6; pp 143–186.

(14) Gorcester, J.; Millhauser, G. L.; Freed, J. H. In *Modern Pulsed and Continuous-Wave Electron Spin Resonance*; Kevan, L., Bowman, M. K., Eds.; Wiley-Interscience: New York, 1990; pp 119–194.

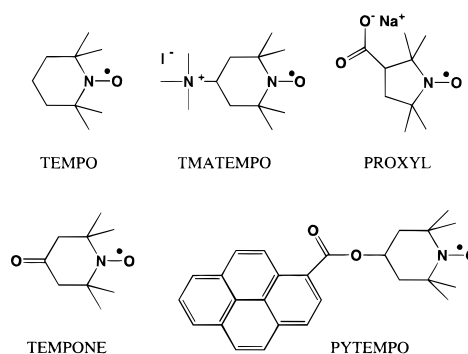
(15) Schweiger, A. *Angew. Chem., Int. Ed. Engl.* **1991**, *30*, 265.

Several experiments described in the literature are designed to exclude the interference of spectral diffusion to a certain extent. The most reliable results are probably obtained with a long-pulse saturation-recovery technique,^{12,13,15–17} in which a long saturating mw pulse allows the spin system to reach a steady state during the preparation period. This leads to a more uniform initial perturbation of a spectrum, which results in a substantial quenching of spectral diffusion. Alternatively, a sequence of short intense pulses and delays can be used for the same purpose.^{15,18} Also, only the latter portions of the recovery traces are often measured^{16,19} and low concentrations of radicals are used to further reduce the influence of spectral diffusion. However, even if a spin system is allowed to achieve a steady state under saturating mw field, a factor of 1.5–2 difference in the true and apparent relaxation times is still possible,¹¹ since under selective mw pumping the steady state does not necessarily correspond to a uniform perturbation. The largest errors are expected when the rates of the spin–lattice relaxation and spectral diffusion are comparable.^{11,20,21}

An alternative approach to measuring spin–lattice relaxation times is a short-pulse saturation-recovery with (in general) a multiexponential fitting of the experimental recovery traces.^{22–25} However, it is usually preferable to deal with single exponential traces, since in many cases the result of a multiexponential fitting of data with the limited signal-to-noise ratio is much less reliable.²⁶ A different but related experimental technique employed in T_1 measurements is a pulsed electron–electron double resonance (ELDOR) experiment,^{13,20,23,24,27} in which an evolution of a given ESR line is monitored after a pulsed perturbation (e.g., inversion) of a second ESR line takes place at a different mw frequency. The resulting traces are described by a sum of at least two exponentials, and a least-squares fitting yields the rates of both the true and competing pseudo-secular relaxation processes. Under conditions when the rate of spectral diffusion is smaller than the spin–lattice relaxation rate, however, the ELDOR signal is weak, and a successful implementation of this technique is not possible.¹⁴ Spin–lattice relaxation time measurements by other experimental techniques, such as cw^{28,29} or pulsed³⁰ longitudinally detected ESR (LODESR), and stimulated (3-pulse) spin echo,^{15,31} are affected by spectral diffusion and thus do not yield the true T_1 time in the case of a non-uniform spectral coverage of the mw pulses.

Thus each of the available techniques requires a certain relation of the rates of spectral diffusion and spin–lattice relaxation (faster, slower, or comparable) for its successful

Scheme 1. Chemical Structures of the Nitroxide Radicals



application. In this work we aimed at developing an experimental procedure free from the interference of spectral diffusion in a wide range of experimental conditions, irrespective of the relative rates of spectral diffusion and spin–lattice relaxation. It is also desirable that a single experiment provides all the necessary data, and that the true T_1 time is evaluated while fitting single-exponential recovery traces, with the latter obtained with minimum or no data manipulation. Since a development of such an experiment for a general case would be unrealistic, we limit ourselves to the case of motionally narrowed ESR spectra of stable nitroxide radicals exhibiting a well-resolved three-line pattern.

We implement and compare two different approaches to exclude the influence of spectral diffusion on the observed recovery traces. Both are based on modifications of a conventional pulsed inversion-recovery scheme. In the first approach it is the preparation period of an experiment which is modified. In this case the goal is to achieve a more uniform initial perturbation of an ESR spectrum under study. We will demonstrate that for the case of motionally narrowed ESR spectra of nitroxide spin labels a uniform inversion of all three ESR lines can be achieved with specially designed pulse trains. We refer to this experiment as RUP (recovery after uniform perturbation). Another possible approach, however, is to modify the detection part of the relaxation-measurement pulse experiment so that it becomes insensitive to pseudo-secular processes even in the case of a non-uniform perturbation. Here we take advantage of the fact that these latter processes only redistribute magnetization among different ESR transitions but do not change the *total* magnetization of the ensemble of radicals. Thus reconstructed recovery of the *total* magnetization (RRTM) is free from pseudo-secular contributions.

We employ the two modified inversion-recovery experiments to obtain a concentration dependence of the T_1 time for benzene solution of TEMPONE. The RRTM approach is also used to study the temperature dependence of T_1 time of TEMPONE and PYTEMPO in both methylcyclohexane (nuclear spin concentrated solvent) and carbon disulfide (nuclear spin dilute solvent) to check the possible involvement of the solvent nuclear spins in the electron spin–lattice relaxation of nitroxide spin labels. Finally, we show preliminary results of the inversion-recovery studies of host–guest interactions for three nitroxide spin labels with CT-DNA and SDS micelles.

2. Experimental Section

Chemicals and Sample Preparation. The structures of nitroxide radicals employed in this study are shown in Scheme 1. TEMPO (2,2,6,6-tetramethyl-1-piperidin-1-yl), TEMPONE (4-oxo-2,2,6,6-tetramethyl-1-piperidin-1-yl), 4-amino-TEMPO (4-amino-2,2,6,6-tetramethyl-1-piperidin-1-yl), PROXYL (3-carboxy-2,2,5,5-tetramethyl-1-pyrrolidin-1-yl), benzene, cyclohexane (spectroscopic grade), carbon disulfide (HPLC grade), Sephadex G25, Trizma, and NaCl were

(16) Percival, P. W.; Hyde, J. S. *J. Magn. Reson.* **1976**, *23*, 249.

(17) Nakagawa, K.; Candelaria, M. B.; Chik, W. W. C.; Eaton, S. S.; Eaton, G. R. *J. Magn. Reson.* **1992**, *98*, 81.

(18) Cheng, C.; Lin, T.-S.; Sloop, D. J. *J. Magn. Reson.* **1979**, *33*, 71.

(19) Kusumi, A.; Subczynski, W. K.; Hyde, J. S. *Proc. Natl. Acad. Sci. U.S.A.* **1982**, *79*, 1854.

(20) Freed, J. H. *J. Phys. Chem.* **1974**, *78*, 1155.

(21) Freed, J. H. In *Time Domain Electron Spin Resonance*; Kevan, L., Schwartz, R. N., Eds.; Wiley-Interscience: New York, 1979; pp 31–66.

(22) Yin, J.-J.; Hyde, J. S. *Z. Phys. Chem. N.F.* **1987**, *153*, 57.

(23) Yin, J.-J.; Pasenkiewicz-Gierula, M.; Hyde, J. S. *Proc. Natl. Acad. Sci. U.S.A.* **1987**, *84*, 964.

(24) Hyde, J. S.; Feix, J. B. In *Biological Magnetic Resonance*; Berliner, L. J., Reuben, J., Eds.; Plenum Press: New York/London, 1989; Vol. 8, pp 305–337.

(25) Hyde, J. S.; Yin, J.-J.; Feix, J. B.; Hubbell, W. L. *Pure Appl. Chem.* **1990**, *62*, 255.

(26) Clayden, N. J.; Hesler, B. D. *J. Magn. Reson.* **1992**, *98*, 271.

(27) Gorchester, J.; Freed, J. H. *J. Chem. Phys.* **1988**, *88*, 4678.

(28) Giordano, M.; Martinelli, M.; Pardi, L.; Santucci, S. *Mol. Phys.* **1981**, *42*, 523.

(29) Giordano, M.; Martinelli, M.; Pardi, L.; Santucci, S.; Umerton, C. *J. Magn. Reson.* **1985**, *64*, 47.

(30) Schweiger, A.; Ernst, R. R. *J. Magn. Reson.* **1988**, *77*, 512.

(31) Salikhov, K. M.; Semenov, A. G.; Tsvetkov, Y. D. *Electron Spin Echoes and Their Applications*; Nauka: Novosibirsk, 1976.

purchased from Aldrich and used as received. Sodium dodecyl sulfate (SDS, Aldrich) was recrystallized from the mixture of diethyl ether and methanol (5:1, v:v). Calf Thymus DNA (CT-DNA) was purchased from Sigma (best quality available) and carefully dialyzed against Trizma buffer, pH 7.2. Other solvents and concentrated hydrochloric acid were purchased from Fisher and were of ACS "certified" quality.

TMATEMPO (2,2,6,6-tetramethyl-1-piperidinyloxy-4-trimethylammonium iodide) was synthesized according to a standard procedure from 4-amino-TEMPO and methyl iodide in DMF³² and further purified by dissolution in water (Millipore) followed by three consequent extractions with methylene chloride. The aqueous phase was evaporated in vacuum at room temperature, and the product was passed through a small chromatography column employing Sephadex G25 as the stationary phase and ethanol as the eluent. PYTEMPO (pyrene-1-(4-oxy-2,2',6,6'-tetramethyl-1-piperidinyloxy)carboxylic acid ester) was synthesized³³ and characterized by elemental analysis (Calcd: C, 77.97; H, 6.544; N, 3.947. Found: C, 77.91; H, 6.52; N, 3.98) and mass spectroscopy (FAB-MS: calcd 400.49; found 401 (0.2%), 58 (100%).

For T_1 concentration dependence measurements various concentrations of TEMPONE in benzene in the range 2.5×10^{-5} M to 10^{-2} M were prepared by dilution of a common stock solution. In variable-temperature experiments the concentration of TEMPONE and PYTEMPO in methylcyclohexane and carbon disulfide was 1.0×10^{-3} M. To compare the spin-lattice relaxation times of nitroxides in various environments the following solutions were prepared. (i) Aqueous solutions: 5 mM Trizma-HCl buffer, pH 7.0, 50 mM NaCl, 2.0×10^{-4} M nitroxides. (ii) CT-DNA solutions: 5 mM Trizma-HCl buffer, pH 7.0, 50 mM NaCl, 1 mM CT-DNA in phosphate units, 2.0×10^{-4} M nitroxides. (iii) SDS: pH 9.0, 100 mM SDS in surfactant molecules, 2.0×10^{-4} M nitroxides. The actual concentration of nitroxides in these samples has been verified by comparing the integrals of their cw ESR spectra with that of a stock solution.

All samples were degassed by at least 4 freeze-pump-thaw cycles and flame-sealed in 5 (quartz or pyrex, nonpolar solvents) or 2 mm o.d. tubes (quartz, aqueous solutions). In order to ensure that the DNA retained its double-stranded structure (B-DNA) in all experiments reported here, the luminescence of the [Ru(phen)₃]²⁺ complex (phen = 1,10-phenanthroline) was monitored for equivalent samples and under equivalent experimental conditions, except that no nitroxides were added. In all cases a double exponential luminescence decay of the ruthenium complex in the presence of DNA has been found, with the typical values of 950 ± 50 ns ($30 \pm 3\%$ of the recorded luminescence decay) for τ_1 and 1900 ± 75 ns ($70 \pm 3\%$) for τ_2 . This control experiment clearly demonstrates that the double-stranded structure of the DNA is retained since the complex does not bind significantly to single-stranded DNA.⁴

Instrumentation. Pulsed ESR experiments were carried out with a Bruker ESP-300/380 pulsed FT ESR spectrometer equipped with a dielectric ring cavity (ESP380-1052 DLQ-H) and a 1 kW TWT amplifier (90° pulse length is 16 ns). A LeCroy 9450A oscilloscope (400 megasamples/s) was used to accumulate complete FIDs, while the dual channel sampling digitizer (SDI) of the ESP-380 instrument was employed in the inversion-recovery and spin-echo experiments. An appropriate phase cycling was performed in all pulsed ESR measurements. To facilitate the decay of an FID in the spin-echo measurements the magnetic field homogeneity was spoiled^{14,34-36} by inserting two rods made of a high- μ material into the holes along the axes of the magnet poles. High pass BHP-25 (3 dB loss at 25 MHz) and low-pass BLP-21.4 (3 dB loss at 24.5 MHz) analog radio frequency filters (Mini-Circuits) were used to separate FIDs corresponding to different ESR lines (*vide infra*).

A CF series helium flow cryostat and a ITC4 temperature controller

(32) Berliner, L. J., Ed. *Spin Labelling: Theory and Applications*; Academic Press: New York/London, 1976; pp 287-291.

(33) Jenks, W. S. Time-Resolved EPR and Photophysical Studies of the Interactions of Doublet and Triplet States with Stable Nitroxides. Ph.D. Thesis, Columbia University, New York, 1991.

(34) Schwartz, R. N.; Jones, L. L.; Bowman, M. K. *J. Phys. Chem.* **1979**, *83*, 3429.

(35) Gorchester, J.; Freed, J. H. *J. Chem. Phys.* **1986**, *85*, 5375.

(36) Bowman, N. K. In *Magnetic Resonance of Carbonaceous Solids*; Botto, R. E., Sanada, Y., Eds.; American Chemical Society: Washington, DC, 1993; Vol. 229, pp 91-105.

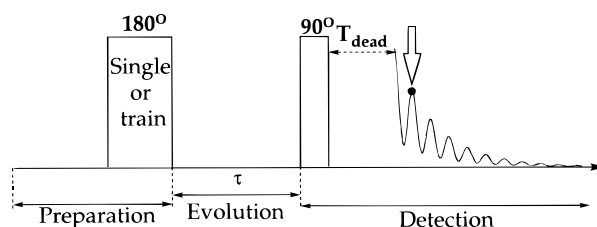


Figure 1. A schematic representation of the general inversion-recovery pulse sequence used in this work. A single point of an FID not affected by a detector deadtime (T_{dead}), as exemplified by the arrow, is used to measure the signal intensity.

(Oxford Instruments) were used in variable-temperature experiments. The ESR cavity with the sample was immersed into the cryostat and cooled by a permanent flow of evaporating helium. The sample was allowed to equilibrate at a desired temperature for at least 1 h, and several T_1 time measurements were performed and discarded until no further change in T_1 time was observed. The accuracy of the temperature readings was 1-2 K.

Data Handling and Calculations. Rotational correlation times of nitroxide spin labels were obtained from the 2-pulse spin-echo decays. The decay times were obtained by single-exponential fitting of the decays for all three nitroxide lines and analyzed in terms of eq 1^{37,38} where $(A:A)$ is the square of the anisotropic part of the hyperfine tensor,

$$1/T_2 = a + bM_1 + cM_1^2$$

$$c = (A:A)[5\tau_R - \tau_R/(1 + \omega^2\tau_R^2)]/60 \quad (1)$$

M_1 is the nitrogen nuclear spin quantum number, and τ_R is the nitroxide rotational correlation time. We note that, strictly speaking, the characteristic decay time of the primary echo should be referred to as "phase memory time T_m ". In many cases in solution the T_m and T_2 times are equal, while we realize that this might be questionable for the lowest temperatures used in the work. However, this has no effect on the evaluation of the rotational correlation times, since only the M_1 -dependent contribution to the T_2 (or T_m) time is used (coefficients c or b in eq 1). We use only coefficient c , and the expression shown is valid for arbitrary $\omega\tau_R$, while in the literature its reduced form for $\omega\tau_R \ll 1$ is usually cited.

The calculations of the excitation patterns for pulse trains were performed in the following way. Each *soft* pulse in a pulse train was approximated by an alternating sequence of N *hard* pulses and delays, $(\phi - \tau)_N$, with the cumulative nominal flip angle $N\phi$ and the duration $N\tau$ equal to those of the soft pulse ($N = 5-20$). The cumulative effect of the sequence of hard pulses and free precession delays was then calculated using the quaternion formalism.³⁹ A 16-ns nominal length of a 90° pulse was used in the calculations. All the pulses were assumed to be rectangular, and relaxation of the spins during the pulse trains was neglected.

The Levenberg-Marquardt least-squares algorithm was employed in single- and double-exponential fitting of the data. Standard deviations are given as the uncertainties of the extracted parameters, where appropriate.

3. Results and Discussion

1. The General Experimental Procedure. The general pulse sequence of our inversion-recovery experiments is shown in Figure 1. It is convenient to distinguish the three periods, preparation, evolution, and detection, as is often done in pulsed nuclear magnetic resonance experiments.⁴⁰ The preparation period starts with a relaxation delay to assure that the mag-

(37) Carrington, A.; McLachlan, A. D. *Introduction to Magnetic Resonance*; Harper & Row: New York, 1967.

(38) Banci, L.; Bertini, I.; Luchinat, C. *Nuclear and Electron Relaxation*; VCH: Weinheim/New York/Basel/Cambridge, 1991.

(39) Bluemich, B.; Spiess, H. W. *J. Magn. Reson.* **1985**, *61*, 356.

(40) Bax, A. *Two-Dimensional Nuclear Magnetic Resonance in Liquids*; Delft University Press: Delft, 1984.

netization of a spin system achieves an equilibrium after a perturbation in a previous cycle. Then at the end of the preparation period the equilibrium magnetization is inverted. In a conventional experiment inversion is achieved by means of a single 180° pulse. However, as discussed below, a single pulse is not always adequate, since an exact inversion occurs only in a limited frequency range, and is sometimes replaced with inverting pulse trains. The evolution period in our case is a variable delay τ which is incremented stepwise in subsequent repetitions of the sequence. During this period the perturbed magnetization recovers to its equilibrium value. The detection period begins with a 90° pulse which tips the partially relaxed magnetization into the transverse plane and thus creates an observable free induction decay (FID) signal. The FID can be detected and Fourier transformed to give an ESR spectrum, and the intensity of an ESR line can be plotted vs τ , which yields a recovery trace. However, in certain cases another strategy can be implemented, namely one can acquire a single point of an FID, keeping the delay between the 90° pulse and acquired point invariable, and use it as a measure of intensity of an ESR line.^{12,41} This is analogous to the electron spin echo (ESE) time-domain experiments in which the echo intensity is monitored at its maximum,^{15,36} considering an echo as a zero-deadtime FID.^{13,42} This way of detecting a recovery trace is justified if either all the ESR lines in the spectrum show the same recovery behavior or if only one ESR line contributes to the observed FID. The latter condition can be readily met for a motionally narrowed ESR spectrum of a nitroxide radical if one of the lines is placed in resonance with the mw field and the bandwidth of the videoamplifier is set to a sufficiently low value (e.g. 25 MHz) to exclude the contributions of the other lines. The detection of a single FID (echo) point reduces dramatically the duration of the experiment, amount of data processing, and memory size for data storage as compared to a conventional experiment with the detection of the whole FID and Fourier transformation. All this allows us to detect a recovery trace with a dwell time of 2 ns or larger and with up to several thousand points in a trace.

2. A Uniform Inversion of the Three-Line ESR Spectrum.

It is a commonly encountered situation in both pulsed NMR and ESR that the spectral range of interest exceeds the "region of hardness" of a single 90° or 180° pulse. The very least outcome of this is the loss of sensitivity at the edges of the detected spectrum, but usually more significant complications can be expected. Numerous attempts are documented in the literature to improve the spectral coverage of pulses for different applications in magnetic resonance.^{43–49} Usually a single pulse is replaced with a pulse sequence (a pulse train) which contains several pulses of different width, phase, and sometimes different magnitude. These parameters and interpulse delays, if any, are computer optimized to achieve the best performance—a broader and more uniform excitation of a spin system and acceptable phase of the induced signal. A fine adjustment of a pulse train can be performed empirically to correct for the effects not taken

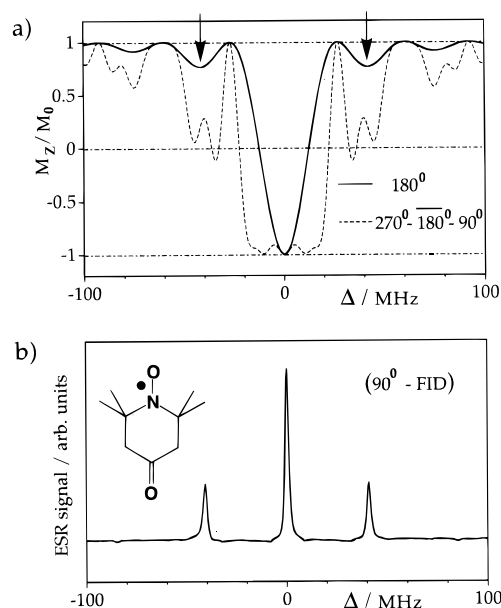


Figure 2. (a) Comparison of the excitation patterns of a single 180° pulse (—) and a composite 180° pulse (---) shown as the relative magnitudes of the M_z magnetization component after the pulse versus the offset from resonance. M_0 is equilibrium magnetization. A 180° -pulse length is taken as 32 ns. Overbar indicates a 180° phase shift of a pulse. Arrows point to the side bands of the excitation patterns. (b) FT ESR spectrum of TEMPONE in benzene at room temperature obtained with a single 90° pulse. The relative line intensities are different from the expected 1:1:1 pattern due to a limited microwave power and a finite Q of the cavity.

into account in the calculations, e.g. non-rectangular pulses, spin relaxation, etc.

However, the excitation bandwidth of a pulse train cannot be increased infinitely for a given power level in the transmitter channel. The attainable limit depends very much on the flexibility of the particular instrument. The pulse trains (or rather, shaped pulses) with the best performance can be designed for instruments where widths, phases, and magnitudes of the pulses can be changed continuously or by small increments.⁴⁹ In pulsed ESR experiments, however, the amplitude of the mw field is usually fixed, because a TWT amplifier is usually operated near the saturation level.^{14,48} Moreover, with the Bruker ESP-380 spectrometer the pulse widths can only be set in multiples of 8 ns and the number of pulse channels (8) limits phase shifts to 45° steps (usually quadrature phase settings 0° , 90° , 180° , 270° are used). This allows us to implement easily the composite 180° (or π) pulses well known in pulsed NMR spectroscopy.^{43,47} Figure 2a compares the performance of a single 180° pulse with that of a $270^\circ_x-180^\circ_{-x}-90^\circ_x$ sequence, showing the much broader frequency range of an almost uniform excitation for the latter. However, to invert uniformly the spectrum of a nitroxide radical (Figure 2b) it would be necessary to design a pulse train with even broader excitation band extending to offsets $\Delta \approx 3\omega_1$, where ω_1 is the magnitude of the mw field in frequency units ($\omega_1 = g\beta B_1/\hbar$) and Δ is the offset from resonance. While the pulse trains with a uniform inversion extending to the offsets as large as $\Delta = 4.7\omega_1$ have been reported,⁴⁸ their implementation requires the flexibility not available with the instrument employed.

Figure 2a also reveals another feature of the pulse trains—the presence of the excitation side bands, or side lobes; they are marked with arrows in the figure. In fact, even a single pulse has these side bands. In designing pulse trains one often ignores them. In certain cases it is necessary to eliminate excitation

(41) Brown, I. M. *J. Chem. Phys.* **1974**, *60*, 4930.

(42) Keijzers, C. P.; Reijerse, E. J.; Schmidt, J.; Eds. *Pulsed EPR: A New Field of Applications*; North Holland: Amsterdam, 1989.

(43) Freeman, R. R.; Kempell, S. P.; Levitt, M. H. *J. Magn. Reson.* **1980**, *38*, 453.

(44) Waugh, J. S. *J. Magn. Reson.* **1982**, *50*, 30.

(45) Levitt, M. H.; Suter, D.; Ernst, R. R. *J. Chem. Phys.* **1984**, *80*, 3064.

(46) Tycko, R.; Schneider, E.; Pines, A. *J. Chem. Phys.* **1984**, *81*, 680.

(47) Levitt, M. H. *Progr. NMR Spectrosc.* **1986**, *18*, 61.

(48) Crepeau, R. H.; Dulcic, A.; Gorcester, J.; Saarinen, T. R.; Freed, J. H. *J. Magn. Reson.* **1989**, *84*, 184.

(49) Kessler, H.; Mronga, S.; Gemmecker, G. *Magn. Reson. Chem.* **1991**, *29*, 527.

side bands,^{50,51} as e.g. in selective excitation sequences or water suppression experiments in ¹H NMR, since they can lead to undesirable perturbations of a spin system. However, for the ESR spectrum of a nitroxide radical in a relatively nonviscous solution with its simple 3-line pattern almost symmetric with respect to its center these side bands can in principle be utilized to invert the $M_I = \pm 1$ components while the main excitation band would invert the $M_I = 0$ component of the spectrum.

The calculated excitation patterns (the relative magnitudes of the M_z magnetization component after applying the pulse train vs the offset from resonance) are shown in Figure 3 for the two pulse trains (eqs 2 and 3) which we used as a starting point

$$45^\circ - 16 \text{ ns} - 45^\circ - 8 \text{ ns} - 45^\circ - 16 \text{ ns} - 45^\circ - 16 \text{ ns} - 45^\circ \quad (2)$$

$$\overline{135^\circ} - 45^\circ - 45^\circ - 8 \text{ ns} - \overline{45^\circ} - 45^\circ \quad (3)$$

(overbar indicates a 180° phase shift of a pulse). Both calculated patterns show excitation maxima at 0 and around ± 45 MHz offsets, matching well the positions of the three ESR lines of TEMPONE radical in nonviscous solution. However, as mentioned in the Experimental Section, the calculations were done for the idealized pulse trains (rectangular pulses, precise timing and phase settings) and did not take into account the relaxation of spins during the pulse train. Thus to achieve acceptable performance a pulse train was further tuned empirically by varying the delays and pulse lengths (only 8-ns increments are possible) and usually repeating several times the whole train or part of it. Finally, to evaluate the performance of a pulse train we compared the ESR spectra of a nitroxide radical detected after a single 90° pulse with that detected after applying the pulse train followed immediately by a 90° pulse. If the train does indeed invert the three lines uniformly, the second spectrum will appear as inversion of the first one. The result of such a comparison for the modification (4) of the pulse train (3) is presented in Figure 4 which shows that the performance is quite satisfactory.

$$\overline{135^\circ} - [45^\circ - \overline{45^\circ} - 8 \text{ ns}]_4 \quad (4)$$

The successful performance of such trains obviously depends on how close the excitation pattern matches the nitroxide triplet. Since the HFI constant of a nitroxide depends on its chemical structure as well as the solvent used, each nitroxide/solvent combination requires its own pulse train for uniform inversion. By varying empirically the interpulse delays (0, 8, or 16 ns, trains (2) and (4)) and the number of pulses (5 or 6 45° pulses, train (2)) we were able to match seven different HFI constants in the range 40.0–47.7 MHz. The approach to achieving uniform inversion described in this section is time-consuming since the performance of such pulse trains is very sensitive to experimental conditions and tuning/matching of the pulsed cavity. Nevertheless, the spin–lattice relaxation time measurements performed employing several pulse trains show that this approach works and gives the true T_1 relaxation times of nitroxides in solution. Some of the results obtained are discussed in sections 3.4 and 3.6. We believe that the design of such pulse trains deserves further development.

3. Reconstructed Recovery of the Total Magnetization.

In the previous section we addressed the preparation period of an inversion recovery experiment. The goal was to achieve a more uniform initial perturbation of an ESR spectrum under study. In such a case the pseudo-secular processes have no apparent effect on a recovery trace, since there is an equal “flux”

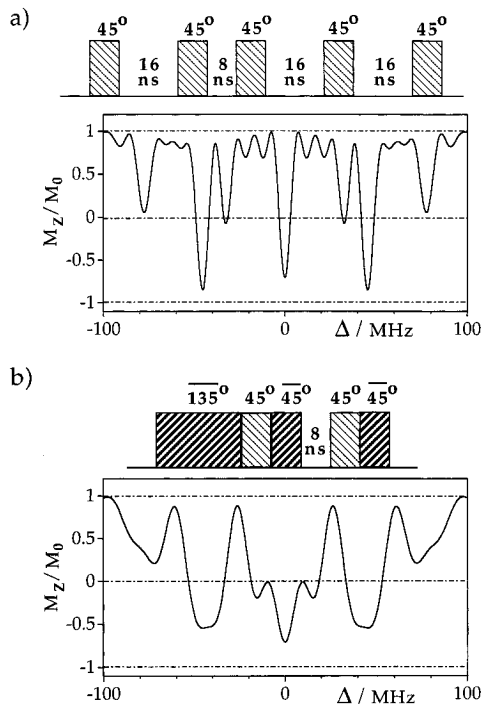


Figure 3. The two pulse trains designed for uniform perturbation of a nitroxide triplet and their excitation patterns. Delays are shown in nanoseconds; 45° pulse is 8 ns long.

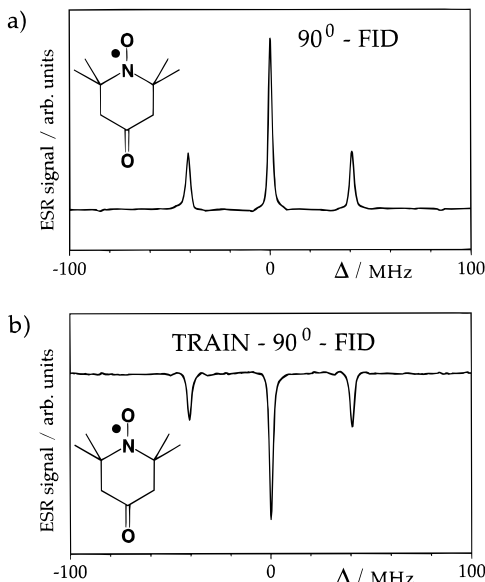


Figure 4. Evaluation of the performance of the inverting pulse train of eq 4. (a) FT ESR spectrum of TEMPONE in solution obtained after Fourier transform of an FID acquired following a single 90° pulse. (b) FT ESR spectrum of the same sample detected with the inverting pulse train of eq 4 immediately preceding the detection 90° pulse.

of magnetization to and from each transition. In this section the detection part of the inversion-recovery experiment is modified instead so that it becomes insensitive to spectral diffusion caused by pseudo-secular processes. The approach is based on the fact that spectral diffusion does not lead to the true spin–lattice relaxation in the sense that it only redistributes magnetization between the three transitions of a nitroxide. On the contrary, spin–lattice relaxation changes the total magnetization of the electron spins involved. Thus if one could monitor the recovery of the total magnetization of all three nitroxide ESR lines the experiment would yield the true T_1 time,^{36,52} even for a non-uniform initial perturbation. Unfortunately, this

(50) Freeman, R. *Chem. Rev.* **1991**, *91*, 1397.

(51) Emsley, L.; Bodenhausen, G. *J. Magn. Reson.* **1992**, *97*, 135.

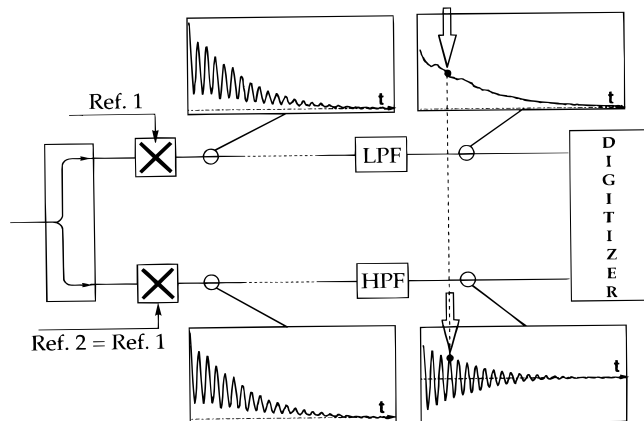


Figure 5. A schematic diagram of the detection scheme modified for the separate detection of the on-resonance $M_I = 0$ line and $M_I = \pm 1$ lines of a nitroxide spin label. LPF = low-pass filter, HPF = high-pass filter; Ref 1 and Ref 2 are the reference input signals of the two mixers (X). One point of each of the two filtered FIDs is detected, as shown by the arrows. For further details see the text.

cannot be done directly. Due to the limited excitation bandwidth of pulses already discussed above and also a limited bandwidth of a cavity with a finite Q value, the sensitivity of a pulsed ESR experiment toward the $M_I = 0$ line placed in resonance and toward the off-resonance $M_I = \pm 1$ lines is different. Thus their relative contributions to an FID are unequal. Besides, different evolution patterns of the three signals in time (simple exponential decay of the on-resonance signal and damped sinusoids for the off-resonance ones, as well as different damping factors due to different line widths) lead to the variation of their relative contributions across the FID. Thus detecting the inversion-recovery trace by monitoring an intensity of any point of the original FID (cf. Figure 1) would give yet another apparent relaxation time T_1^{obs} rather than the true T_1 time. Since we do not want to discard the basic scheme of the experiment outlined above in section 3.1, it definitely has to be modified.

The strategy employed was to separate the contributions of the $M_I = 0$ line and $M_I = \pm 1$ lines first, detect independent recovery traces for the two separated signals, and then combine them with appropriate weights. The separation can be achieved quite easily. In the detection system of the FT ESR spectrometer the mw signal is split and fed into two mixers for detection⁴² (Figure 5). Usually the reference inputs of the two mixers differ in phase by 90° for the quadrature detection of an FID. Fortunately, the design of the spectrometer allows one to adjust the phases of the two channels independently. In our experiment the two channels have the same reference phase, i.e. the same FID appears in both detection channels. To separate the contributions we install two analog RF filters between the mixers and the digitizer. One channel contains a low-pass filter (LPF) rejecting frequencies higher than the cut-off frequency (ca. 25 MHz), and thus only the contribution from the $M_I = 0$ line placed in resonance reaches the digitizer (Figure 5). Another contains a high-pass (band-pass) filter (HPF) rejecting low-frequency signals (below ca. 25 MHz) and thus selecting the contributions of $M_I = \pm 1$ lines. With this configuration after applying a 180° inversion pulse at zero frequency (in resonance with the $M_I = 0$ line) the two recovery traces for the $M_I = 0$ and $M_I = \pm 1$ lines can be detected separately in a single experiment monitoring the intensity of the two separated FIDs at the same point in time (cf. Figure 5).

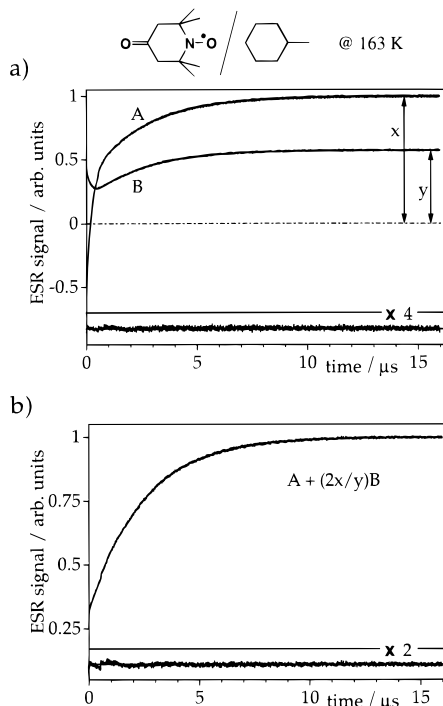


Figure 6. (a) The recovery of the on-resonance $M_I = 0$ line (A) and the off-resonance $M_I = \pm 1$ lines (B) of TEMPONE in methylcyclohexane at 163 K after a perturbation with a single 180° pulse. Relative intensities of traces A and B are shown as detected. The inset shows the difference of trace B and its double-exponential fit. (b) Reconstructed recovery of the total magnetization. The inset demonstrates the quality of its single-exponential fit. A slight discontinuity at 560 ns (the longest interpulse delay for which the two pulses are amplified within a single TWT duty cycle) is caused by phase properties of the TWT amplifier⁷³ and is present on all traces to a certain extent.

An example of the application of the procedure outlined above is shown in Figure 6a. The two recovery traces A and B have been detected for 1 mM TEMPONE in methylcyclohexane at 163 K with a single 180° pulse used for inversion. For both traces a considerable deviation from a simple exponential behavior is obvious, which in this case is caused by fast nuclear relaxation often observed for nitroxides in viscous media^{20,23–25,53} (see, however, the paper by Zhong and Pilbrow⁵⁴). Trace A is identical to that obtained in a conventional two-pulse inversion-recovery experiment. Trace B is similar to those obtained in pulsed electron–electron double resonance (ELDOR) experiments.^{14,53,55,56} The signal intensity of trace B at $t = 0$ is lower than the equilibrium value since the inversion 180° pulse affects the off-resonance lines to a certain extent. Fast nuclear spin relaxation transfers perturbation from the on-resonance line to the less perturbed off-resonance lines. This results in the initial decrease of trace B and the fast initial rise of trace A. After a common spin temperature is established throughout the spin system, both traces evolve toward thermal equilibrium at a slower rate.

We now proceed with the reconstruction of the recovery of the total magnetization. The two traces A and B are added together in such a proportion that their relative contributions at $t = \infty$ ($t \gg T_1$) are 1:2, equal to the relative statistic weights of $M_I = 0$ and $M_I = \pm 1$ radical ensembles. The reconstructed recovery trace ($A + (2x/y)B$) is shown in Figure 6b, and it

(53) Hyde, J. S.; Froncisz, W.; Mottley, C. *Chem. Phys. Lett.* **1984**, *110*, 621.

(54) Zhong, Y. C.; Pilbrow, J. R. *J. Magn. Reson. A* **1995**, *112*, 109.

(55) Mailer, C.; Robinson, B. H.; Haas, D. A. *Bull. Magn. Reson.* **1992**, *14*, 30.

(56) Robinson, B. H.; Haas, D. A.; Mailer, C. *Science* **1994**, *263*, 490.

(52) Kababya, S.; Luz, Z.; Goldfarb, D. *J. Am. Chem. Soc.* **1994**, *116*, 5805.

represents the recovery of the entire ensemble of spins and is quite close to a single exponential behavior with $T_1 = 2409 \pm 2$ ns.

The separate detection of the on-resonance and off-resonance recovery traces at low temperatures (cf. Figure 6a) provides an independent test for our RRTM method. The two traces A and B are expected⁵³ to exhibit double exponential behavior with the same characteristic times $\tau_1 = T_1$ and $\tau_2 = (1/T_1 + 3W_n)^{-1}$. Here T_1 is the true electron spin–lattice relaxation time and W_n is the probability of a nuclear spin transition, which for a $I = 1$ nuclear spin system is related³⁷ to the nuclear spin relaxation time T_1^n as $W_n = 1/T_1^n$. Double-exponential fitting of traces A and B is expected to be quite accurate, for electron and nuclear relaxation under these conditions have comparable contributions to these traces, while the individual rates of the two processes are substantially different. The values $T_1 = 2450 \pm 6$ ns, ($\tau_1 = T_1$) and $T_1^n = 718 \pm 5$ ns ($\tau_2 = 218 \pm 1$ ns) for the on-resonance ($M_I = 0$) line and $T_1 = 2412 \pm 5$ ns and $T_1^n = 697 \pm 8$ ns ($\tau_2 = 212 \pm 2$ ns) for the off-resonance ($M_I = \pm 1$) lines were obtained from the double exponential fittings of traces A and B (Figure 6a), respectively, which is in very good agreement with the value obtained above from the single-exponential fit of the reconstructed recovery trace and with the literature data (*vide infra*). It was found, however, that the reconstruction method works equally well under a variety of experimental conditions, including those where a double-exponential fit does not provide reliable results. For instance, at ambient temperatures Heisenberg spin exchange leads to a noticeable spectral diffusion even at relatively low nitroxide concentrations (*vide infra*). Reconstruction of the recovery of the total magnetization eliminates the effect of spectral diffusion and yields single-exponential recovery traces in all experiments performed in this work.

It is important to note that a successful application of the experimental procedure outlined above requires that all the hyperfine components of the ESR spectrum have similar T_1 times, otherwise some weighted average will be measured. The same, however, is true about the majority of the other spin–lattice relaxation techniques,¹³ and even for the inversion-recovery with uniform perturbation, RUP, described in section 3.2. Fortunately, it has been shown for several nitroxide spin labels under various experimental conditions that T_1 times of different hyperfine lines are indeed very close,^{16,24,28} which is also in agreement with the T_1 values obtained above.

Thus a single and relatively simple experiment contains all the necessary information to reconstruct the behavior of the total electron spin magnetization of an ensemble of nitroxide radicals in solution and thus exclude the interference of spectral diffusion. Its implementation requires that the spectrum under study is in the motionally narrowed regime, and that the on-resonance and off-resonance ensembles can be distinguished and detected separately. We have verified experimentally that even under the most unfavorable conditions used in this work (TEMPONE in methylcyclohexane at 153 K, $\tau_R = 380$ ps) the three lines can be distinguished in the ESR spectrum of a nitroxide radical, despite a substantial line broadening, especially pronounced for the low-frequency (high-field, $M_I = -1$) line.

4. The Concentration Dependence of T_1 . To experimentally test the two proposed modifications of the inversion-recovery experiment we have studied the concentration dependence of TEMPONE spin–lattice relaxation time T_1 in benzene at room temperature and compared the results with the literature data. The T_1 times measured using the RRTM and RUP methods are shown in Figure 7. At nitroxide concentrations higher than 1 mM spectral diffusion becomes fast enough to

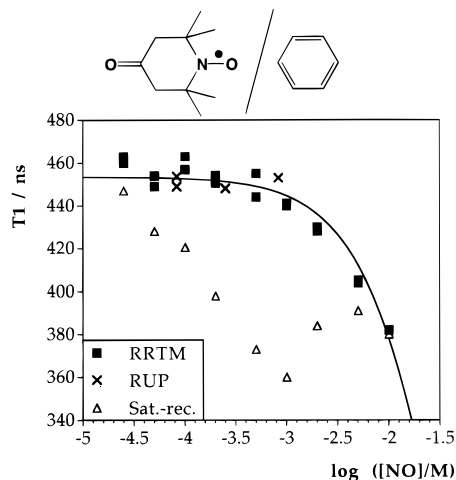


Figure 7. Concentration dependence of the spin–lattice relaxation time measured for TEMPONE (labeled NO in the figure) in benzene at room temperature. The results of the RRTM (■), RUP (×) and saturation-recovery (△) experiments are shown. The solid line shows the best fit to RRTM data assuming a linear dependence of relaxation rate on nitroxide concentration (see text).

significantly affect magnetization evolution during the inverting pulse train (4) with total duration of 120 ns, which can cause the uniform inversion to fail. For this reason the RUP method was not applied at higher concentrations. The first important conclusion that can be made is that the T_1 times measured with two methods are essentially the same even in the concentration region where the influence of spin exchange is strongest (*vide infra*). Given the different principles of the two experiments, this finding strongly supports our expectation that a true T_1 time is obtained in these experiments. The variation of T_1 with nitroxide concentration is then rationalized in a straightforward way. The only (intermolecular) processes which potentially contribute to the T_1 concentration dependence are the spin exchange and dipole–dipole interaction of electron spins. Of these only the non-secular part of the intermolecular dipole–dipole interaction is expected to alter the true T_1 time, since other contributions have a pseudo-secular nature. Thus at low nitroxide concentrations ($<10^{-3}$ M) the T_1 time is almost concentration independent, for the rate of the intermolecular dipolar relaxation is too slow to compete with the intramolecular relaxation pathways. At higher concentrations the T_1 time decreases reflecting the faster intermolecular process, and this allows us to estimate the rate constant of non-secular dipole–dipole relaxation. Assuming that the intermolecular relaxation rate is proportional to nitroxide concentration,^{16,28,31} the fitting of experimental data (Figure 7) yields $1/T_{dd} = [(4.4 \pm 0.2) \times 10^7] C \text{ s}^{-1}$, where C is the concentration of TEMPONE. A value of the same order of magnitude can be deduced from Figure 4 of the paper by Giordano *et al.*²⁸

For comparative purposes Figure 7 also shows the results obtained in a saturation-recovery experiment (triangles). In this case a $(90^\circ - 200 \text{ ns})_N$ sequence with $N = 8 - 20$ was employed for a prolonged saturation, followed by a variable delay and a probe 90° pulse. As before, a single point of an FID was detected, and the T_1 times were obtained from single-exponential fitting of the whole recovery traces. As was mentioned in the introduction, fitting of the tails of the recovery traces obtained in the saturation-recovery experiment should give a somewhat better quantitative agreement with our inversion-recovery data, while the qualitative behavior would still be the same. For concentrations of TEMPONE around 10^{-3} M the deviation of the experimental traces from the single exponential behavior was pronounced, but still less than that for a conventional

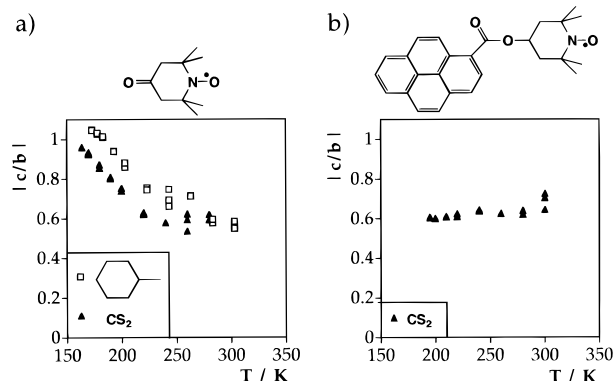


Figure 8. Temperature dependence of the absolute c/b ratio, calculated according to eq 1 from the T_2 times measured in the two-pulse spin-echo experiments: (a) TEMPONE in methylcyclohexane (\square) and carbon disulfide (\blacktriangle); (b) PYTEMPO in carbon disulfide.

inversion-recovery trace, since a long saturating pulse train partially quenches the spectral diffusion. The variation of the apparent time T_1^{obs} measured in the saturation-recovery experiment with concentration is different from that discussed above, but can be readily rationalized²⁰ if we assume that the effect of spin exchange is not completely quenched, as expected. When the radical concentration is low, the different ESR lines are not coupled by the exchange interaction, and the recovery of a perturbed ESR line occurs only due to the true spin-lattice relaxation. This means that in the limit of zero TEMPONE concentration the saturation-recovery experiment should yield the true T_1 time. This is clearly what is observed in the experiment, though even at the lowest concentration studied (2.5×10^{-5} M) the T_1^{obs} is still slightly lower than T_1 . At the same time, at high radical concentrations the coupling of the ESR lines due to spin exchange is so efficient that the uniform spin temperature in the spin system is established very rapidly and is maintained throughout the recovery process. Thus in the limit of high concentrations of TEMPONE the apparent relaxation time also tends to the true T_1 , again in agreement with observation. It is clear that the deviation of T_1^{obs} from T_1 is maximized at some intermediate concentrations, when the spin-lattice relaxation and spectral diffusion have comparable rates. According to Figure 7, this happens at concentrations around 10^{-3} M. This allows us to estimate the rate of intermolecular spin exchange as 2.2×10^{-9} C s⁻¹. This is in agreement with the conclusions found in the literature^{14,24,57-59} that the rate of spin exchange in solution is usually comparable with the rate of bimolecular collisions of radicals.

The value of T_1 extrapolated to zero TEMPONE concentration is found to be 455 ± 2 ns, very close to $T_1 = 470$ ns measured by Percival and Hyde for 5×10^{-5} M perdeuterio-TEMPONE in *sec*-butylbenzene.¹⁶ This comparison is justified by the fact that spin-lattice relaxation of nitroxides is rather insensitive to isotope substitution and is almost the same for all hyperfine lines,^{16,24} although some small differences could arise due to a different solvent.¹¹ A similar value ($T_1 < 500$ ns) was obtained by Schwartz *et al.*³⁴ in a saturation-recovery experiment with an echo detection for perdeuterio-TEMPONE in perdeuteriotoluene at room temperature, as can be deduced from Figure 8 of their paper. The authors also report an absence of any noticeable dependence of T_1 on nitroxide concentration in the range 10^{-4} to 3.5×10^{-3} M. In our experiments this

variation amounts to ca. 10% of the T_1 extrapolated to zero concentration, probably reflecting a higher accuracy of our data. In fact, if only one nitroxide line is inverted, as in the experiments of Schwartz *et al.*,³⁴ an even larger variation of T_1^{obs} is to be expected. It is, however, impossible to make a more detailed comparison, since their work is mainly devoted to a careful study of T_2 times, and does not give a detailed description of T_1 measurements.

Giordano *et al.*²⁸ have studied the T_1 concentration dependence of TEMPONE in toluene for an unusually wide concentration range, 2.5×10^{-4} to 5 M, by a combination of cw ESR and LODER techniques. In the low-concentration range the values of T_1 obtained almost coincide with those measured in a cw saturation experiment, and thus are not free from pseudo-secular contributions. This was taken into account in the quantitative analysis of the data,²⁸ and a value of $T_1 = 570$ ns was obtained from an extrapolation to zero concentration. This value is somewhat higher than those reported in the other papers and measured in this work, and is probably overestimated due to a limited number of points in the low-concentration range, since the largest value actually measured was ca. 300 ns (350 ns in cw saturation experiments).

We conclude that the two modifications of the inversion-recovery experiment developed in this work give the results consistent with the data obtained in the other, independent measurements described in the literature. This finding is encouraging enough to proceed with practical applications of these techniques.

5. The Temperature Dependence of T_1 . We have employed our RRTM technique to study the temperature dependence of the T_1 time of TEMPONE in order to address the question about the mechanism of spin-lattice relaxation in nitroxides, which remains to be a controversial issue in the literature.^{11,16,24,55,56} In particular, we aimed at experimentally testing the recent statement^{55,56} that spin-lattice relaxation measurements can be rationalized assuming isotropic Brownian rotational and translational motion of a nitroxide spin label, if along with spin-rotation and electron-nuclear dipolar interaction another relaxation mechanism, termed "spin diffusion", is taken into account. The essence of this latter mechanism is the existence of a pool of interacting nuclear spins (e.g., of hydrogen atoms) of a solvent bulk and a coupling of the nuclear spins with the electron spin of a nitroxide modulated by translational motion. Since the nature of the latter coupling is not specified, the variation of the contribution of this mechanism with the isotope labeling of a solvent cannot be predicted. Thus the only way to examine the validity of the proposed explanation is to design an experiment where the effect of spin diffusion is excluded altogether, i.e. a solvent is used which does not contain any magnetic nuclei. To do that we have compared the dependence of the nitroxide spin label T_1 times in methylcyclohexane and carbon disulfide (CS₂). The latter is a good approximation for a "spinless" solvent, since the natural abundances of the magnetic isotopes of carbon (¹³C, 1.1%) and sulfur (³³S, 0.75%) are very low. Thus, switching from methylcyclohexane to carbon disulfide corresponds to almost a 1000-fold reduction in the concentration of magnetic nuclei of a solvent and is expected to eliminate any solvent-induced relaxation.

To directly compare the T_1 times measured in two different solvents the corresponding rotational correlation times have been determined. The latter can in principle be estimated from the Stokes-Einstein equation, since the viscosity of methylcyclohexane⁶⁰ and carbon disulfide⁶¹ at various temperatures has been

(57) Hyde, J. S.; Chien, J. C. W.; Freed, J. H. *J. Chem. Phys.* **1968**, *48*, 4211.

(58) Davis, M. S.; Mao, C.; Kreilick, R. W. *Mol. Phys.* **1975**, *29*, 665.

(59) Molin, Y. N.; Salikhov, K. M.; Zamaraev, K. I. *Spin Exchange*; Springer-Verlag: Berlin, 1980.

(60) Ruth, A. A.; Nickel, B.; Lesche, H. Z. *Phys. Chem.* **1992**, *175*, 91.

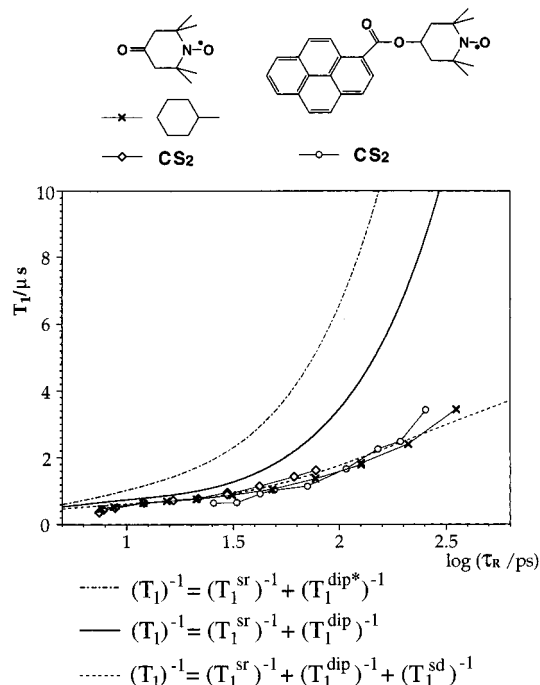


Figure 9. The dependence of the spin–lattice relaxation time T_1 on the rotational correlation time. Experimental data for TEMPONE in methylcyclohexane (x), carbon disulfide (◊), and PYTEMPO in carbon disulfide (○). The dashed line shows the best fit of the experimental data (x) with eqs 5 and 6 with R^{sd} as the only variable parameter. The solid line shows the contribution of the first two terms in eq 5. The dot-dashed line shows the same, but with the dipolar contribution ($T_1^{\text{dip}*}$) calculated according to Robinson *et al.*⁵⁶

reported. However, when the T_1 times for different spin labels are compared, we found that more accurate results are obtained, if the rotational correlation times are determined from the analysis of the hyperfine-dependent part of the spin–spin relaxation time T_2 according to eq 1.³⁷ This has a further advantage that the character of motion of the spin label can be deduced from the analysis of the temperature dependence of the $|c/b|$ ratio.⁶² Figure 8a shows the results obtained for TEMPONE in methylcyclohexane and CS_2 . The behavior is very similar to that found by Hwang *et al.*⁶² for perdeuterio-TEMPONE in toluene: for $\tau_R > 10^{-10}$ s $|c/b|$ is close to 1.0, but drops to ca. 0.6 for $\tau_R < 10^{-11}$ s, which was shown to be consistent with the isotropic tumbling of the nitroxide. The two data sets in Figure 8a appear to be shifted relative to each other, reflecting the fact that the viscosity of CS_2 is lower than that of methylcyclohexane at the same temperature.⁶¹ The tumbling of another nitroxide, PYTEMPO (Scheme 1), is quite different, as expected. As can be concluded from Figure 8b, for this nitroxide the $|c/b|$ ratio is constant over the temperature range studied, which according to Hwang *et al.*⁶² implies an anisotropic tumbling of the spin label. This observation is clearly in agreement with the structure of PYTEMPO, which favors anisotropic rotation around the ester tether. Nevertheless, this modified tumbling has only a small effect on the T_1 time of the nitroxide (*vide infra*).

The T_1 times of TEMPONE and PYTEMPO obtained from the single-exponential fitting of the reconstructed recovery traces are shown in Figure 9 as a function of rotational correlation time τ_R . The results are very close to the results of Percival and Hyde.¹⁶ Although not shown, the T_1 time for PYTEMPO

in methylcyclohexane shows very similar behavior. It is obvious that the increase in the T_1 time of TEMPONE with an increase in the rotational correlation time is almost the same in methylcyclohexane and CS_2 . The range of TEMPONE τ_R values for the latter solvent in the temperature interval studied is much narrower than that for methylcyclohexane. The use of PYTEMPO allowed us to further slow down the tumbling of the spin label and to almost completely match the range of τ_R studied in the two solvents. This range is much narrower than that studied in refs 55 and 56, mainly because this work is primarily concerned with developing and testing the techniques described above, and the latter are no longer applicable directly at higher viscosities. Nevertheless, this range is wide enough for the purposes of the comparison.

It is clear from the results of Figure 9 that the T_1 times in the two solvents are very close. Some small variations can be caused by numerous factors, including various experimental uncertainties as well as differences related to the spin labels and solvents. However, the observed variations are negligible as compared to what one should expect, if spin diffusion was operative in one solvent and not in the other. The combined action of spin-rotation, electron–nuclear dipolar interaction, and spin diffusion (the three mechanisms which according to Mailer *et al.*⁵⁵ and Robinson *et al.*⁵⁶ can account for the observed relaxation times) is described by the following equation:

$$1/T_1 = 1/T_1^{\text{sr}} + 1/T_1^{\text{dip}} + 1/T_1^{\text{sd}} \quad (5)$$

where^{38,56}

$$1/T_1^{\text{sr}} = \sum (g_i - g_e)^2 / (9\tau_R); \quad i = x, y, z$$

$$1/T_1^{\text{dip}} =$$

$$(1/30)(7I(I+1) - M_I^2) \sum (A_i - A_0)^2 \tau_R / (1 + \omega^2 \tau_R^2)$$

$$1/T_1^{\text{sd}} = R^{\text{sd}} [2\omega \tau_R / (1 + (\omega \tau_R)^{1.5})]^{0.25} \quad (6)$$

The quantity T_{1e}^{END} used in the work of Robinson *et al.*⁵⁶ is the same as our $T_1^{\text{dip}*}$, while the expression for T_1^{dip} is a more general and corrected form for the electron spin–lattice relaxation due to electron–nuclear dipolar interaction. As defined earlier in the text, M_I is the spin quantum number of a nitroxide nitrogen atom with nuclear spin I . The best fit of our experimental data with eqs 5 and 6 is shown with a dashed line in Figure 9, with R^{sd} being the only variable parameter of the fit. The solid curve shows the contribution of the first two terms of eq 5 to the T_1 time. The two curves show the scale of the expected difference of the relaxation behavior in the two solvents, if solvent nuclear spins were indeed involved in the relaxation. Moreover, for the upper limit of the τ_R range studied in this work, at least an order of magnitude increase in the T_1 time in CS_2 is predicted from Figure 3 of the paper by Mailer *et al.*⁵⁵ This is clearly not what is observed experimentally. Thus, no experimental evidence was found of the involvement of the nuclear spins of a solvent in the relaxation of nitroxide spin labels in solution.

6. T_1 Times of Nitroxide Spin Labels in Some Microheterogeneous Environments. While the main goal of this work was to establish and test the reliable experimental procedures for measuring accurate values of nitroxide spin–lattice relaxation times by the modified inversion-recovery techniques, it was tempting to check if these techniques would indeed be useful in studying systems of current interest. In particular, we are interested in probing supramolecular microheterogeneous systems such as micelles and polyions. Below we report the

(61) Viswanath, D. S.; Natarajan, G. *Data Book on the Viscosity of Liquids*; Hemisphere Publishing Corp.: New York, 1989.

(62) Hwang, J. S.; Mason, R. P.; Hwang, L.-P.; Freed, J. H. *J. Phys. Chem.* **1975**, *79*, 489.

Table 1. Spin–Lattice Relaxation Times of the Three Nitroxide Radicals Measured in Various Environments^a

| | T_1 /ns | | |
|------------------|-----------|----------|--------|
| | TEMPO | TMATEMPO | PROXYL |
| H ₂ O | 695 | 685 | 845 |
| SDS | 630 | 1560 | 945 |
| CT-DNA | 630 | 680 | 900 |

^a The structures of the radicals are shown in Scheme 1. The values shown are accurate to $\pm 5\%$.

preliminary measurements of the T_1 relaxation times for three differently charged nitroxide radicals and two microheterogeneous systems: sodium dodecyl sulfate micelles and B-DNA.

Micelles are of great interest because they are widely used in basic research as well as in many technical applications.⁶³ A micelle consists of a hydrophobic core formed by the aliphatic chains and a negatively charged boundary region which is formed by the polar head groups. Depending on the chain length of the aliphatic groups and the concentration of the surfactant monomers in the system, different aggregation numbers can be found. For SDS micelles the aggregation number for the concentrations used in these experiments is between 85 and 100.^{64,65}

B-DNA represents the most abundant form of DNA. In contrast to a globular dynamic structure of micelles, DNA is relatively rigid and possesses a rod-like shape.⁶⁶ Among the significant features of the DNA structure are the major and the minor grooves with different abilities to bind charged and noncharged particles such as metal complexes and proteins, and the negative charges along the helical backbone which make it a polyelectrolyte. As required by its molecular structure, there are two negatively charged phosphate groups per DNA base pair. The determination of the binding properties of differently charged compounds to B-DNA and the mobility of water (solvent) molecules in proximity to the DNA structure are of special interest for the design of drugs, especially of anti-cancer nature.⁶⁷

Both SDS micelles and B-DNA have an electrical double layer, which is formed by the immobile negative charges imbedded in their structures and the mobile electrically compensating counterions (e.g., sodium). The structure of the electrical double layer depends on the total concentration of ions in the microheterogeneous systems. Whereas at higher concentrations (>0.1 M) a compact double layer can be formed (model of Helmholtz), at lower concentrations a combination of a compact and a diffuse double layer describes the observed behavior (model of Stern).⁶⁷ According to this paradigm a positively charged nitroxide (TMATEMPO) should bind more strongly to both B-DNA and micelles than a neutral nitroxide. Furthermore, a negatively charged nitroxide (PROXYL) should be repelled by the microheterogeneous structure. Deviations from this simple scheme should be found in the cases where hydrophobic interactions play a dominant role.

Table 1 summarizes the T_1 relaxation times measured for TMATEMPO, TEMPO, and PROXYL in the presence of SDS micelles and CT-DNA. Aqueous solutions of the nitroxides served as a reference system. As becomes immediately clear

from the table, SDS binds TMATEMPO significantly leading to more than a 2-fold increase in the T_1 relaxation time. In agreement with our working paradigm, the values for TEMPO and PROXYL remain almost unchanged in comparison to those of water. Interestingly, no significant interaction of all three spin probes with B-DNA has been detected. Nevertheless, our control experiment (see Experimental Section) clearly demonstrated that the DNA was intact during our measurements. Therefore we conclude that the binding of all three spin probes to DNA is apparently weak and that the mobility of the water in proximity to the DNA's structure is high. This experiment provides some insights into the structure of the electrical layer around DNA. Higher charged compounds such as ruthenium(II) and rhodium(III) complexes possessing planar organic ligands are strongly bound by intercalation.⁶⁸ Compounds with a single positive charge possess a high mobility next to DNA comparable to their mobilities in the water bulk. This finding strongly supports the existence of a diffuse electrical layer around the polyelectrolyte DNA.

Another observation concerns the mechanism of spin–lattice relaxation of nitroxide radicals. Apparently the relaxation times for both six-membered-ring nitroxides are very similar, whereas the value found for the five-membered ring is significantly larger. These different relaxation behaviors can be related to the different motion characteristics of five- and six-membered-ring systems: in five-membered rings an envelope conformation is dominant, but in six-membered rings chair conformations and subsequently occurring ring interconversions are found leading to a faster motion.⁶⁹ The possibility that the spin–lattice relaxation in nitroxides is dominated by intramolecular motional modes was recognized in the literature^{11,16,62} and cannot be discarded altogether while the main relaxation mechanism remains unknown.

4. Concluding Remarks

In this work we have demonstrated that the inversion-recovery experiment can be successfully applied to the spin–lattice relaxation time measurements of nitroxide spin labels, if it is modified to prevent the interference of spectral diffusion. Our first approach (RUP) is to use triply-selective pulse trains, which possess an excitation pattern matching the motionally narrowed three-line ESR spectrum of a nitroxide radical, and thus provide an almost uniform initial perturbation of the spectrum. In the second approach (RRTM) we combine the conventional inversion-recovery technique for the central line with the pulsed ELDOR technique for the two outer lines, in one experiment, and eventually reconstruct the recovery of the total magnetization of the ensemble of radicals which is not affected by spectral diffusion.

Obviously, a much more straightforward way to measure the T_1 times of nitroxide spin labels would be the conventional inversion-recovery experiment with mw pulses short and powerful enough to invert the entire motionally narrowed ESR spectrum. At present this is not possible with the commercial instruments, for the required incident mw power grows as a cube of the spectral coverage of a pulse.^{27,48} Progress in the field of pulsed ESR will eventually lead to higher mw fields available commercially. In the meantime, the techniques proposed in this work might prove useful in carrying out reliable spin–lattice relaxation measurements under constraints of limited mw power.

(63) Rosen, M. J. *Surfactants and Interfacial Phenomena*; John Wiley & Sons: New York/Chichester/Brisbane/Toronto, 1989.

(64) Myers, D. *Surfaces, Interfaces and Colloids: Principles and Applications*; Verlag Chemie: Weinheim, 1991.

(65) Dörfler, H.-D. *Grenzflächen und Kolloidchemie*; Verlag Chemie: Weinheim, 1994.

(66) Saenger, W. *Principles of Nucleic Acid Structure*; Springer-Verlag: New York/Berlin/Heidelberg/London/Paris/Tokyo, 1988.

(67) Turro, N. J.; Barton, J. K.; Tomalia, D. A. *Acc. Chem. Res.* **1991**, *24*, 332.

(68) Murphy, C. J.; Arkin, M. R.; Ghatlia, N. D.; Turro, N. J.; Barton, J. K. *Proc. Natl. Acad. Sci. U.S.A.* **1994**, *91*, 5315.

(69) Christen, R. In *Principles of Organic Chemistry*; Otto Salle-Verlag: Frankfurt (Main), 1982; pp 89–101.

One can take advantage of the improved accuracy of T_1 measurements to reveal subtle changes in relaxation behavior. For instance, in this work it allowed us to conclude that nuclear spins of a solvent do not contribute noticeably to the electron spin–lattice relaxation in nitroxide radicals. While we are unaware of any other nitroxide spin–lattice relaxation studies in a “spinless” solvent, this conclusion is in accord with the literature findings that there are only minor differences in T_1 times measured in different solvents of comparable viscosity.²⁴ However, a careful systematic study of spin–lattice relaxation times for a wide range of solvents was, in fact, never attempted. It could, in principle, reveal the importance of other aspects of solute–solvent interaction, if minor variations of the T_1 times were reliably detected.

Both RUP and RRTM methods have substantial limitations of their applicability discussed in the preceding sections of this work. In principle, it should be possible to extend these methods to other radicals exhibiting simple hyperfine patterns. However, given the present hardware limitations of the design of composite pulses, the feasibility of the uniform inversion in the RUP experiment should be specifically studied for a particular radical in question. The RRTM approach essentially relies on the invariance of the spin–lattice relaxation time across the ESR spectrum of a radical. Both approaches are applicable only in the fast motional limit. In our variable-temperature study of nitroxide T_1 times we have almost reached the limit of applicability for the RRTM approach. While some advance to larger rotational correlation times is still possible, the reliability of the results will suffer due to a substantial broadening of the high-field nitroxide ESR line and the resulting loss of sensitivity due to a significant signal decay within the spectrometer deadtime.

Our RRTM experiment is in fact a close relative of the ELDOR technique, and can be used as such. Since the

introduction of loop-gap resonators it became clear that the two mw frequencies necessary for ELDOR experiments can be accommodated within the same cavity.²⁵ It was also demonstrated that in a pulsed ELDOR experiment one mw pulse produces all combinations of pump and probe frequencies, and a two-dimensional Fourier transform can easily separate them.¹⁴ In our RRTM experiment we use analog filters to separate the responses from various ESR lines. While analog filters are useful in many applications of magnetic resonance,⁷⁰ an obvious improvement would be to implement digital filtering of data, which is now routinely used in NMR spectroscopy^{71,72} and easily outperforms analog filtering in many respects. Much like in modern NMR, the digital filtering of ESR data can be performed on the fly despite much higher repetition rates usually employed, if the filtering is done while a sampling oscilloscope performs an extensive averaging of an FID for the next step of a phase cycle. This improvement in data acquisition and manipulation will provide a very simple way of detecting one-dimensional pulsed ELDOR traces for measuring the rates of spectral diffusion due to nuclear spin relaxation, spin exchange, etc.

Acknowledgment. This work was supported by grants from NSF, KAST (Kanagawa Academy of Science and Technology, Japan), DFG (Deutsche Forschungsgemeinschaft), and Hewlett Packard. We thank Professor David C. Doetschman (SUNY, Binghamton) for help in mastering the practical aspects of pulsed ESR spectroscopy and for helpful discussions.

JA952152D

(70) Skinner, T. E.; Pruski, J.; Robitaille, P.-M. *J. Magn. Reson.* **1992**, *98*, 604.

(71) Rosen, M. E. *J. Magn. Reson. A* **1994**, *107*, 119.

(72) Craven, C. J.; Waltho, J. P. *J. Magn. Reson. B* **1995**, *106*, 40.

(73) Bowman, M. K. In *Modern Pulsed and Continuous-Wave Electron Spin Resonance*; Kevan, L., Bowman, M. K., Eds.; Wiley-Interscience: New York, 1990; pp 1–42.